

# The Discontinuous Enrichment Method (DEM) for Multi-Scale Transport Problems

**Irina Kalashnikova\***

Ph.D. Candidate

Institute for Computational & Mathematical Engineering (iCME)  
Stanford University

Sandia National Laboratories  
Albuquerque, NM

John von Neumann Research Fellowship Interview Seminar  
Monday, February 7, 2011

\* Joint work with Prof. Charbel Farhat and Dr. Radek Tezaur (Department of Aeronautics & Astronautics, Stanford University).



# Outline

- 1 Motivation
- 2 Advection-Diffusion Equation
- 3 Discontinuous Enrichment Method (DEM)
- 4 DEM for Constant-Coefficient Advection-Diffusion
  - Enrichment Bases
  - Lagrange Multiplier Approximations
  - Element Design
  - Numerical Experiments
- 5 DEM for Variable-Coefficient Advection-Diffusion
  - Enrichment Bases
  - Lagrange Multiplier Approximations
  - Element Design
  - Numerical Experiments
- 6 Extension of DEM to Unsteady, Non-Linear Problems
- 7 Summary



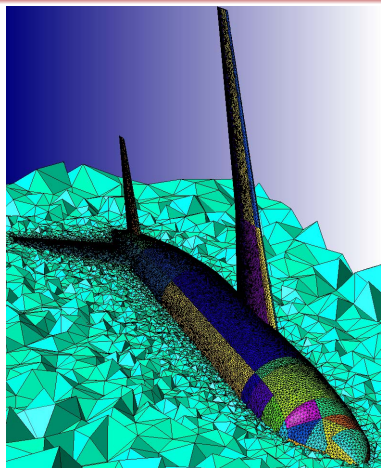
# Outline

- 1 Motivation
- 2 Advection-Diffusion Equation
- 3 Discontinuous Enrichment Method (DEM)
- 4 DEM for Constant-Coefficient Advection-Diffusion
  - Enrichment Bases
  - Lagrange Multiplier Approximations
  - Element Design
  - Numerical Experiments
- 5 DEM for Variable-Coefficient Advection-Diffusion
  - Enrichment Bases
  - Lagrange Multiplier Approximations
  - Element Design
  - Numerical Experiments
- 6 Extension of DEM to Unsteady, Non-Linear Problems
- 7 Summary



# The Finite Element Method (FEM) in Fluid Mechanics

- Galerkin **Finite Element Method** (FEM) has a number of attractions in fluid mechanics:
  - Flexibility in handling complex geometries.
  - Ability to handle different forms of boundary conditions.
- FEM is quasi-optimal for elliptic (*diffusion-dominated*) PDEs: assures good performance of the computation at any mesh resolution.

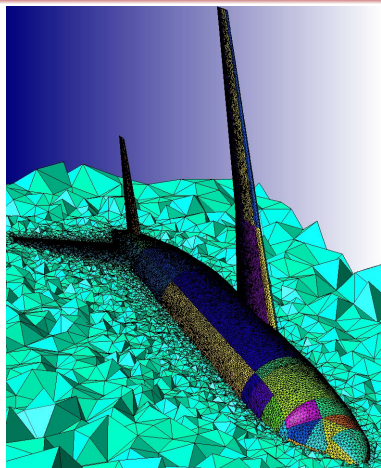


# The Finite Element Method (FEM) in Fluid Mechanics

- Galerkin **Finite Element Method** (FEM) has a number of attractions in fluid mechanics:
  - Flexibility in handling complex geometries.
  - Ability to handle different forms of boundary conditions.
- FEM is quasi-optimal for elliptic (*diffusion-dominated*) PDEs: assures good performance of the computation at any mesh resolution.

## However:

coarse mesh accuracy is not guaranteed when the flow is *advection-dominated*!



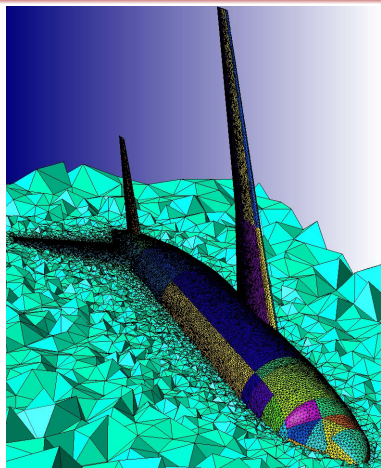
# The Finite Element Method (FEM) in Fluid Mechanics

- Galerkin **Finite Element Method** (FEM) has a number of attractions in fluid mechanics:
  - Flexibility in handling complex geometries.
  - Ability to handle different forms of boundary conditions.
- FEM is quasi-optimal for elliptic (*diffusion-dominated*) PDEs: assures good performance of the computation at any mesh resolution.

## However:

coarse mesh accuracy is not guaranteed when the flow is *advection-dominated*!

Significant mesh refinement typically needed to capture boundary layer region



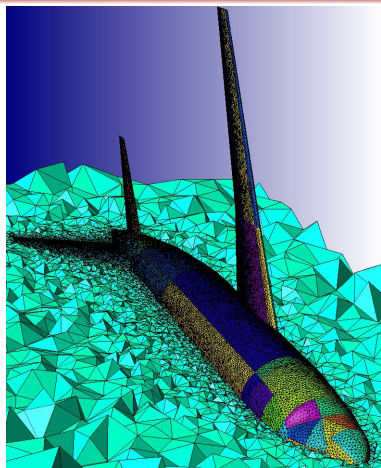
# The Finite Element Method (FEM) in Fluid Mechanics

- Galerkin **Finite Element Method** (FEM) has a number of attractions in fluid mechanics:
  - Flexibility in handling complex geometries.
  - Ability to handle different forms of boundary conditions.
- FEM is quasi-optimal for elliptic (*diffusion-dominated*) PDEs: assures good performance of the computation at any mesh resolution.

## However:

coarse mesh accuracy is not guaranteed when the flow is *advection-dominated*!

Significant mesh refinement typically needed to capture boundary layer region



**EXPENSIVE!**



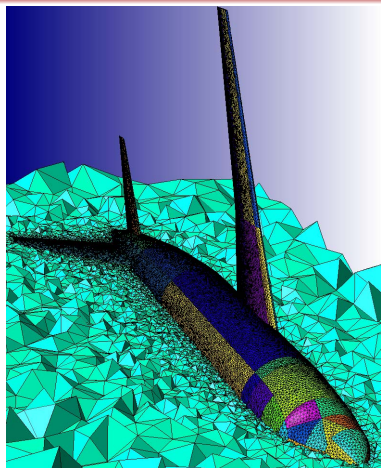
# The Finite Element Method (FEM) in Fluid Mechanics

- Galerkin **Finite Element Method** (FEM) has a number of attractions in fluid mechanics:
  - Flexibility in handling complex geometries.
  - Ability to handle different forms of boundary conditions.
- FEM is quasi-optimal for elliptic (*diffusion-dominated*) PDEs: assures good performance of the computation at any mesh resolution.

## However:

coarse mesh accuracy is not guaranteed when the flow is *advection-dominated*!

Significant mesh refinement typically needed to capture boundary layer region



**EXPENSIVE!**

- **Goal:** build an efficient method that can accurately capture boundary layers.
- **Approach:** start with simple canonical equation; then generalize.



# Outline

- 1 Motivation
- 2 Advection-Diffusion Equation
- 3 Discontinuous Enrichment Method (DEM)
- 4 DEM for Constant-Coefficient Advection-Diffusion
  - Enrichment Bases
  - Lagrange Multiplier Approximations
  - Element Design
  - Numerical Experiments
- 5 DEM for Variable-Coefficient Advection-Diffusion
  - Enrichment Bases
  - Lagrange Multiplier Approximations
  - Element Design
  - Numerical Experiments
- 6 Extension of DEM to Unsteady, Non-Linear Problems
- 7 Summary



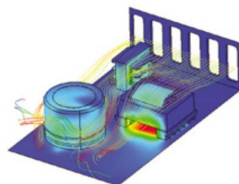
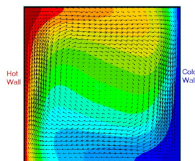
# 2D Scalar Advection-Diffusion Equation

$$\mathcal{L}c = \underbrace{-\kappa \Delta c}_{\text{diffusion}} + \underbrace{\mathbf{a} \cdot \nabla c}_{\text{advection}} = f$$

- Advection velocity:

$$\mathbf{a} = (a_1, a_2)^T = |\mathbf{a}|(\cos \phi, \sin \phi)^T.$$

- $\phi$  = advection direction.
- $\kappa$  = diffusivity.



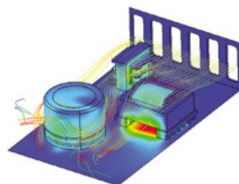
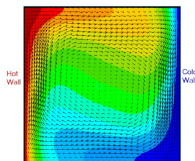
- Describes many transport phenomena in fluid mechanics:
  - Heat transfer.
  - Semi-conductor device modeling.
  - Usual scalar model for the more challenging Navier-Stokes equations.



# 2D Scalar Advection-Diffusion Equation

$$\mathcal{L}c = \underbrace{-\kappa \Delta c}_{\text{diffusion}} + \underbrace{\mathbf{a} \cdot \nabla c}_{\text{advection}} = f$$

- Advection velocity:  
 $\mathbf{a} = (a_1, a_2)^T = |\mathbf{a}|(\cos \phi, \sin \phi)^T$ .
- $\phi$  = advection direction.
- $\kappa$  = diffusivity.



- Describes many transport phenomena in fluid mechanics:
  - Heat transfer.
  - Semi-conductor device modeling.
  - Usual scalar model for the more challenging Navier-Stokes equations.
- Global **Péclet number** ( $L$  = length scale associated with  $\Omega$ ):

$$Pe = \frac{\text{rate of advection}}{\text{rate of diffusion}} = \frac{L|\mathbf{a}|}{\kappa} = Re \cdot \begin{cases} Pr & \text{(thermal diffusion)} \\ Sc & \text{(mass diffusion)} \end{cases}$$



# Advection-Dominated Regime

- Typical applications: flow is advection-dominated.

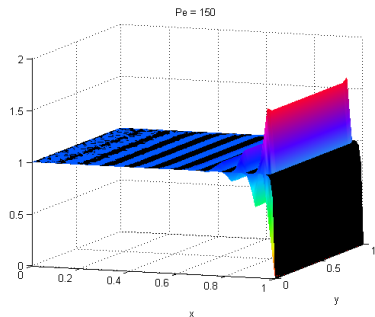


**Figure 1:** Galerkin  $Q_1$  solution (color) vs. exact solution (black) for  $Pe = 150$

Advection-Dominated  
(High  $Pe$ ) Regime  
 $\Downarrow$   
 Sharp gradients in exact solution  
 $\Downarrow$   
 Galerkin FEM inadequate:  
 spurious oscillations (Fig. 1)

- Some classical remedies:
  - Stabilized FEMs** (SUPG, GLS, USFEM): add weighted residual (numerical diffusion) to variational equation.
  - RFB, VMS, PUM**: construct conforming spaces that incorporate knowledge of local behavior of solution.



# Outline

- 1 Motivation
- 2 Advection-Diffusion Equation
- 3 Discontinuous Enrichment Method (DEM)**
- 4 DEM for Constant-Coefficient Advection-Diffusion
  - Enrichment Bases
  - Lagrange Multiplier Approximations
  - Element Design
  - Numerical Experiments
- 5 DEM for Variable-Coefficient Advection-Diffusion
  - Enrichment Bases
  - Lagrange Multiplier Approximations
  - Element Design
  - Numerical Experiments
- 6 Extension of DEM to Unsteady, Non-Linear Problems
- 7 Summary



# The Discontinuous Enrichment Method (DEM)

## Idea of DEM:

“Enrich” the usual Galerkin polynomial field  $\mathcal{V}^P$  by the free-space solutions to the governing homogeneous PDE  $\mathcal{L}c = 0$ .

$$c^h = c^P + c^E \in \mathcal{V}^P \oplus (\mathcal{V}^E \setminus \mathcal{V}^P)$$

where

$$\mathcal{V}^E = \text{span}\{c : \mathcal{L}c = 0\}$$

- **Simple 1D Example:**

$$\begin{cases} u_x - u_{xx} = 1 + x, & x \in (0, 1) \\ u(0) = 0, u(1) = 1 \end{cases}$$

- *Enrichments:*  $u_x^E - u_{xx}^E = 0 \Rightarrow u^E = C_1 + C_2 e^x \Rightarrow \mathcal{V}^E = \text{span}\{1, e^x\}$ .
- *Galerkin FEM polynomials:*  $\mathcal{V}_{\Omega^e=(x_j, x_{j+1})}^P = \text{span}\left\{\frac{x_{j+1}-x}{h}, \frac{x-x_j}{h}\right\}$ .



# History of DEM's Success

- **Acoustic scattering problems** (Helmholtz equation) [4,5].
  - First developed by Farhat *et. al* in 2000 for the Helmholtz equation.
  - A family of 3D hexahedral DEM elements for medium frequency problems achieved the same solution accuracy as Galerkin elements of comparable convergence order using 4–8 times fewer dofs, and *up to 60 times less CPU time* [4].
  - Numerically scalable domain decomposition-based iterative solver for 2D and 3D acoustic scattering problems in medium- and high-frequency regimes has been developed [5].
- **Wave propagation in elastic media** (Navier's equation) [6].
- **Fluid-structure interaction problems** (Navier's equation and the Helmholtz equation) [7, 8].



# History of DEM's Success

- **Acoustic scattering problems** (Helmholtz equation) [4,5].
  - First developed by Farhat *et. al* in 2000 for the Helmholtz equation.
  - A family of 3D hexahedral DEM elements for medium frequency problems achieved the same solution accuracy as Galerkin elements of comparable convergence order using 4–8 times fewer dofs, and *up to 60 times less CPU time* [4].
  - Numerically scalable domain decomposition-based iterative solver for 2D and 3D acoustic scattering problems in medium- and high-frequency regimes has been developed [5].
- **Wave propagation in elastic media** (Navier's equation) [6].
- **Fluid-structure interaction problems** (Navier's equation and the Helmholtz equation) [7, 8].

Excellent performance motivates  
development of DEM for other applications  
→ **Fluid Mechanics**



# Two Variants of DEM

- Two variants of DEM: “**pure DGM**” vs. “**true DEM**”

	DGM	DEM
$\mathcal{V}^h$	$\mathcal{V}^E$	$\mathcal{V}^P \oplus (\mathcal{V}^E \setminus \mathcal{V}^P)$
$c^h$	$c^E$	$c^P + c^E$

## Enrichment-Only “Pure DGM”:

Contribution of the standard polynomial field is dropped entirely from the approximation.

## True or “Full” DEM:

Splitting of the approximation into coarse (polynomial) and fine (enrichment) scales.

- Unlike PUM, VMS & RFB: enrichment field in DEM is not required to vanish at element boundaries



# Two Variants of DEM

- Two variants of DEM: “**pure DGM**” vs. “**true DEM**”

	DGM	DEM
$\mathcal{V}^h$	$\mathcal{V}^E$	$\mathcal{V}^P \oplus (\mathcal{V}^E \setminus \mathcal{V}^P)$
$c^h$	$c^E$	$c^P + c^E$

## Enrichment-Only “Pure DGM”:

Contribution of the standard polynomial field is dropped entirely from the approximation.

## True or “Full” DEM:

Splitting of the approximation into coarse (polynomial) and fine (enrichment) scales.

- Unlike PUM, VMS & RFB: enrichment field in DEM is not required to vanish at element boundaries  $\Rightarrow$  DEM is **discontinuous** by construction!

DEM = DGM with Lagrange Multipliers



# What about Inter-Element Continuity?

- Continuity across element boundaries is enforced weakly using Lagrange multipliers  $\lambda^h \in \mathcal{W}^h$ :

$$\lambda^h \approx \nabla c_{\theta^e}^E \cdot \mathbf{n}^e = -\nabla c_{\theta^{e'}}^E \cdot \mathbf{n}^{e'} \quad \text{on } \Gamma^{e,e'}$$

*but making sure we uphold the...*

- Discrete **Babuška-Brezzi *inf-sup* condition**<sup>1</sup>:

$$\left\{ \begin{array}{l} \# \text{ Lagrange multiplier} \\ \text{constraint equations} \end{array} \leq \begin{array}{l} \# \text{ enrichment} \\ \text{equations} \end{array} \right\}$$

Rule of thumb to satisfy the Babuška-Brezzi *inf-sup* condition is to limit:

$$n^\lambda = \left\lfloor \frac{n^E}{4} \right\rfloor \equiv \max \left\{ n \in \mathbb{Z} \mid n \leq \frac{n^E}{4} \right\}$$

$$n^\lambda = \# \text{ Lagrange multipliers per edge}$$

$$n^E = \# \text{ enrichment functions}$$

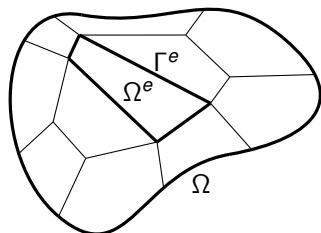
<sup>1</sup>Necessary condition for generating a non-singular global discrete problem. 



# Hybrid Variational Formulation of DEM

- Strong form:

$$(S) : \left\{ \begin{array}{l} \text{Find } \mathbf{c} \in H^1(\Omega) \text{ such that} \\ -\kappa \Delta \mathbf{c} + \mathbf{a} \cdot \nabla \mathbf{c} = f, \quad \text{in } \Omega \\ \mathbf{c} = g, \quad \text{on } \Gamma = \partial\Omega \end{array} \right.$$



## Notation:

$$\tilde{\Omega} = \bigcup_{e=1}^{n_{el}} \Omega^e$$

$$\tilde{\Gamma} = \bigcup_{e=1}^{n_{el}} \Gamma^e$$

$$\Gamma^{e,e'} = \Gamma^e \cap \Gamma^{e'}$$

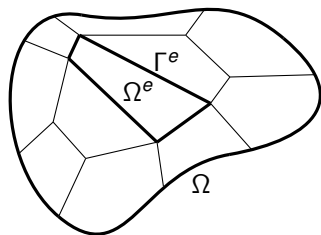
$$\Gamma^{\text{int}} = \bigcup_{e' < e} \bigcup_{e=1}^{n_{el}} \{ \Gamma^e \cap \Gamma^{e'} \}$$



## Hybrid Variational Formulation of DEM

- Strong form:

$$(S) : \left\{ \begin{array}{l} \text{Find } c \in H^1(\Omega) \text{ such that} \\ -\kappa \Delta c + \mathbf{a} \cdot \nabla c = f, \quad \text{in } \Omega \\ c = g, \quad \text{on } \Gamma = \partial\Omega \\ c_e - c_{e'} = 0, \quad \text{on } \Gamma^{\text{int}} \end{array} \right.$$



## Notation:

$$\tilde{\Omega} = \bigcup_{e=1}^{n_{el}} \Omega^e$$

$$\tilde{\Gamma} = \bigcup_{e=1}^{n_{el}} \Gamma^e$$

$$\Gamma^{e,e'} = \Gamma^e \cap \Gamma^{e'}$$

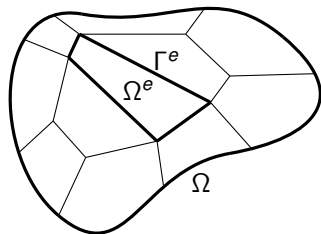
$$\Gamma^{\text{int}} = \bigcup_{e' < e} \bigcup_{e=1}^{n_{el}} \{ \Gamma^e \cap \Gamma^{e'} \}$$



# Hybrid Variational Formulation of DEM

- Strong form:

$$(S) : \begin{cases} \text{Find } c \in H^1(\Omega) \text{ such that} \\ -\kappa \Delta c + \mathbf{a} \cdot \nabla c = f, & \text{in } \Omega \\ c = g, & \text{on } \Gamma = \partial\Omega \\ c_e - c_{e'} = 0, & \text{on } \Gamma^{\text{int}} \end{cases}$$



- Weak hybrid variational form:

$$(W) : \begin{cases} \text{Find } (c, \lambda) \in \mathcal{V} \times \mathcal{W} \text{ such that:} \\ a(v, c) + b(\lambda, v) = r(v) \\ b(\mu, c) = -r_d(\mu) \\ \text{holds } \forall c \in \mathcal{V}, \forall \mu \in \mathcal{W}. \end{cases}$$

where

$$a(v, c) = (\kappa \nabla v + \mathbf{v} \mathbf{a}, \nabla c)_{\tilde{\Omega}}$$

$$b(\lambda, v) = \sum_e \sum_{e' < e} \int_{\Gamma^{e,e'}} \lambda (v_{e'} - v_e) d\Gamma + \int_{\Gamma} \lambda v d\Gamma$$

**Notation:**

$$\tilde{\Omega} = \bigcup_{e=1}^{n_{el}} \Omega^e$$

$$\tilde{\Gamma} = \bigcup_{e=1}^{n_{el}} \Gamma^e$$

$$\Gamma^{e,e'} = \Gamma^e \cap \Gamma^{e'}$$

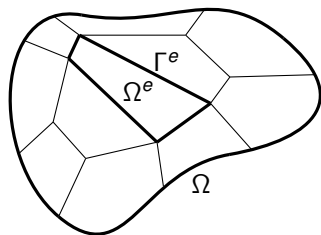
$$\Gamma^{\text{int}} = \bigcup_{e' < e} \bigcup_{e=1}^{n_{el}} \{ \Gamma^e \cap \Gamma^{e'} \}$$



## Hybrid Variational Formulation of DEM

- Strong form:

$$(S) : \begin{cases} \text{Find } c \in H^1(\Omega) \text{ such that} \\ -\kappa \Delta c + \mathbf{a} \cdot \nabla c = f, & \text{in } \Omega \\ c = g, & \text{on } \Gamma = \partial\Omega \\ c_e - c_{e'} = 0, & \text{on } \Gamma^{\text{int}} \end{cases}$$



- Weak hybrid variational form:

$$(W) : \begin{cases} \text{Find } (c, \lambda) \in \mathcal{V} \times \mathcal{W} \text{ such that:} \\ a(v, c) + b(\lambda, v) = r(v) \\ b(\mu, c) = -r_d(\mu) \\ \text{holds } \forall c \in \mathcal{V}, \forall \mu \in \mathcal{W}. \end{cases}$$

where

$$a(v, c) = (\kappa \nabla v + \mathbf{v} \mathbf{a}, \nabla c)_{\tilde{\Omega}}$$

$$b(\lambda, v) = \sum_e \sum_{e' < e} \int_{\Gamma^{e,e'}} \lambda (v_{e'} - v_e) d\Gamma + \int_{\Gamma} \lambda v d\Gamma$$

Notation:

$$\tilde{\Omega} = \bigcup_{e=1}^{n_{el}} \Omega^e$$

$$\tilde{\Gamma} = \bigcup_{e=1}^{n_{el}} \Gamma^e$$

$$\Gamma^{e,e'} = \Gamma^e \cap \Gamma^{e'}$$

$$\Gamma^{\text{int}} = \bigcup_{e' < e} \bigcup_{e=1}^{n_{el}} \{ \Gamma^e \cap \Gamma^{e'} \}$$



# Discretization & Implementation

- Element matrix problem (uncondensed):

$$\begin{pmatrix} \mathbf{k}^{PP} & \mathbf{k}^{PE} & \mathbf{k}^{PC} \\ \mathbf{k}^{EP} & \mathbf{k}^{EE} & \mathbf{k}^{EC} \\ \mathbf{k}^{CP} & \mathbf{k}^{CE} & \mathbf{0} \end{pmatrix} \begin{pmatrix} \mathbf{c}^P \\ \mathbf{c}^E \\ \lambda^h \end{pmatrix} = \begin{pmatrix} \mathbf{r}^P \\ \mathbf{r}^E \\ \mathbf{r}^C \end{pmatrix}$$



# Discretization & Implementation

- Element matrix problem (uncondensed):

$$\begin{pmatrix} \mathbf{k}^{PP} & \mathbf{k}^{PE} & \mathbf{k}^{PC} \\ \mathbf{k}^{EP} & \mathbf{k}^{EE} & \mathbf{k}^{EC} \\ \mathbf{k}^{CP} & \mathbf{k}^{CE} & \mathbf{0} \end{pmatrix} \begin{pmatrix} \mathbf{c}^P \\ \mathbf{c}^E \\ \lambda^h \end{pmatrix} = \begin{pmatrix} \mathbf{r}^P \\ \mathbf{r}^E \\ \mathbf{r}^C \end{pmatrix}$$

Due to the discontinuous nature of  $\mathcal{V}^E$ ,  $\mathbf{c}^E$  can be eliminated at the element level by a static condensation



# Discretization & Implementation

- Element matrix problem (uncondensed):

$$\begin{pmatrix} \mathbf{k}^{PP} & \mathbf{k}^{PE} & \mathbf{k}^{PC} \\ \mathbf{k}^{EP} & \mathbf{k}^{EE} & \mathbf{k}^{EC} \\ \mathbf{k}^{CP} & \mathbf{k}^{CE} & \mathbf{0} \end{pmatrix} \begin{pmatrix} \mathbf{c}^P \\ \mathbf{c}^E \\ \lambda^h \end{pmatrix} = \begin{pmatrix} \mathbf{r}^P \\ \mathbf{r}^E \\ \mathbf{r}^C \end{pmatrix}$$

Due to the discontinuous nature of  $\mathcal{V}^E$ ,  $\mathbf{c}^E$  can be eliminated at the element level by a static condensation

- Statically-condensed **True DEM Element**:

$$\begin{pmatrix} \tilde{\mathbf{k}}^{PP} & \tilde{\mathbf{k}}^{PC} \\ \tilde{\mathbf{k}}^{CP} & \tilde{\mathbf{k}}^{CC} \end{pmatrix} \begin{pmatrix} \mathbf{c}^P \\ \lambda^h \end{pmatrix} = \begin{pmatrix} \tilde{\mathbf{r}}^P \\ \tilde{\mathbf{r}}^C \end{pmatrix}$$

- Statically-condensed **Pure DGM Element**:

$$-\mathbf{k}^{CE} (\mathbf{k}^{EE})^{-1} \mathbf{k}^{EC} \lambda^h = \mathbf{r}^C - \mathbf{k}^{CE} (\mathbf{k}^{EE})^{-1} \mathbf{r}^E$$



# Discretization & Implementation

- Element matrix problem (uncondensed):

$$\begin{pmatrix} \mathbf{k}^{PP} & \mathbf{k}^{PE} & \mathbf{k}^{PC} \\ \mathbf{k}^{EP} & \mathbf{k}^{EE} & \mathbf{k}^{EC} \\ \mathbf{k}^{CP} & \mathbf{k}^{CE} & \mathbf{0} \end{pmatrix} \begin{pmatrix} \mathbf{c}^P \\ \mathbf{c}^E \\ \lambda^h \end{pmatrix} = \begin{pmatrix} \mathbf{r}^P \\ \mathbf{r}^E \\ \mathbf{r}^C \end{pmatrix}$$

Computational complexity depends on  $\dim \mathcal{V}^h$  not on  $\dim \mathcal{V}^E$

Due to the discontinuous nature of  $\mathcal{V}^E$ ,  $\mathbf{c}^E$  can be eliminated at the element level by a static condensation

- Statically-condensed **True DEM Element**:

$$\begin{pmatrix} \tilde{\mathbf{k}}^{PP} & \tilde{\mathbf{k}}^{PC} \\ \tilde{\mathbf{k}}^{CP} & \tilde{\mathbf{k}}^{CC} \end{pmatrix} \begin{pmatrix} \mathbf{c}^P \\ \lambda^h \end{pmatrix} = \begin{pmatrix} \tilde{\mathbf{r}}^P \\ \tilde{\mathbf{r}}^C \end{pmatrix}$$

- Statically-condensed **Pure DGM Element**:

$$-\mathbf{k}^{CE} (\mathbf{k}^{EE})^{-1} \mathbf{k}^{EC} \lambda^h = \mathbf{r}^C - \mathbf{k}^{CE} (\mathbf{k}^{EE})^{-1} \mathbf{r}^E$$



# Outline

- 1 Motivation
- 2 Advection-Diffusion Equation
- 3 Discontinuous Enrichment Method (DEM)
- 4 DEM for Constant-Coefficient Advection-Diffusion**
  - Enrichment Bases
  - Lagrange Multiplier Approximations
  - Element Design
  - Numerical Experiments
- 5 DEM for Variable-Coefficient Advection-Diffusion
  - Enrichment Bases
  - Lagrange Multiplier Approximations
  - Element Design
  - Numerical Experiments
- 6 Extension of DEM to Unsteady, Non-Linear Problems
- 7 Summary



# Angle-Parametrized Enrichment Functions for 2D Advection-Diffusion

- Derived by solving  $\mathcal{L}c^E = \mathbf{a} \cdot \nabla c^E - \kappa \Delta c^E = 0$  analytically (e.g., separation of variables).

$$c^E(\mathbf{x}; \theta_i) = e^{\left(\frac{a_1 + |\mathbf{a}| \cos \theta_i}{2\kappa}\right)(x - x_{r,i})} e^{\left(\frac{a_2 + |\mathbf{a}| \sin \theta_i}{2\kappa}\right)(y - y_{r,i})} \quad (1)$$

$\mathbf{a}^T \equiv (a_1, a_2) =$  advection velocity vector

$(x_{r,i}, y_{r,i}) =$  reference point for  $c_i^E$

$\Theta^c \equiv \{\theta_i\}_{i=1}^{n^E} \in [0, 2\pi) =$  set of angles specifying  $\mathcal{V}^E$

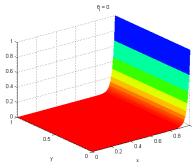
The parametrization with respect to  $\theta_i$  in (1) is non-trivial!

- Enrichment functions are now specified by a set of “flow directions”.
- Parametrization enables systematic element design.

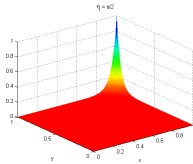


# Plots of Enrichment Functions for Some Angles

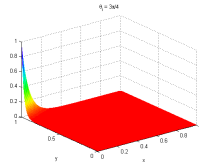
$$\theta_i \in [0, 2\pi)$$



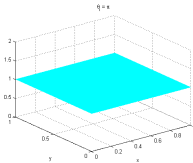
$$\phi = 0, \theta_i = 0$$



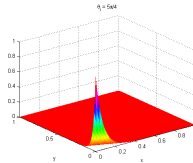
$$\phi = 0, \theta_i = \frac{\pi}{2}$$



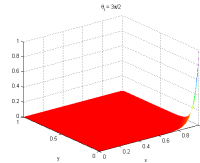
$$\phi = \frac{\pi}{2}, \theta_i = \frac{3\pi}{4}$$



$$\phi = 0, \theta_i = \pi$$



$$\phi = \frac{3\pi}{2}, \theta_i = \frac{5\pi}{4}$$



$$\phi = 0, \theta_i = \frac{3\pi}{2}$$

Figure 2: Plots of enrichment function  $c^E(\mathbf{x}; \theta_i)$  for several values of  $\theta_i$  ( $Pe = 20$ )



# What about the Lagrange Multiplier Approximations?

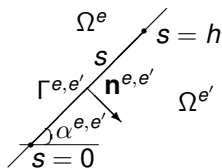


Figure 3: Straight edge  $\Gamma^{e,e'}$  oriented at angle  $\alpha^{e,e'} \in [0, 2\pi)$

- Trivial to compute given exponential enrichments:

$$\begin{aligned} \lambda^h(\mathbf{s})|_{\Gamma^{e,e'}} &\approx \nabla \mathbf{c}^E \cdot \mathbf{n}|_{\Gamma^{e,e'}} \\ &= \mathit{const} \cdot \mathbf{e} \left\{ \frac{|\mathbf{a}|}{2\kappa} [\cos(\phi - \alpha^{e,e'}) + \cos(\theta_k - \alpha^{e,e'})] (s - s_r^{e,e'}) \right\} \end{aligned}$$



# What about the Lagrange Multiplier Approximations?

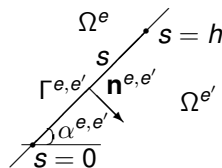


Figure 3: Straight edge  $\Gamma^{e,e'}$  oriented at angle  $\alpha^{e,e'} \in [0, 2\pi)$

- Trivial to compute given exponential enrichments:

$$\begin{aligned} \lambda^h(\mathbf{s})|_{\Gamma^{e,e'}} &\approx \nabla \mathbf{c}^E \cdot \mathbf{n}|_{\Gamma^{e,e'}} \\ &= \text{const} \cdot \mathbf{e} \left\{ \frac{|\mathbf{a}|}{2\kappa} [\cos(\phi - \alpha^{e,e'}) + \cos(\theta_k - \alpha^{e,e'})] (s - s_r^{e,e'}) \right\} \end{aligned}$$

Non-trivial to satisfy *inf-sup* condition:  
the set  $\Theta^c$  that defines  $\mathcal{V}^E$  typically leads to  
too many Lagrange multiplier dofs!



# Lagrange Multiplier Selection

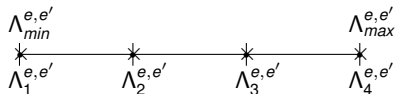


Illustration of Lagrange Multiplier selection for  $n^\lambda = 4$

- Define:

$$\Lambda_i^{e,e'} \equiv \frac{|\mathbf{a}|}{2\kappa} \left[ \cos(\phi - \alpha^{e,e'}) + \cos(\theta_k - \alpha^{e,e'}) \right]$$

$\Downarrow$

$$\lambda^h|_{\Gamma^{e,e'}} = \text{span} \left\{ e^{\Lambda_i^{e,e'}(s - s_{r,i}^{e,e'})}, 0 \leq s \leq h \right\}$$

- Determine # Lagrange multipliers allowed:  $\text{card}\{\Lambda_i^{e,e'}\} = \left\lfloor \frac{n^E}{4} \right\rfloor$ .
- Sample  $\Lambda_i^{e,e'}$  uniformly in the interval  $[\Lambda_{min}^{e,e'}, \Lambda_{max}^{e,e'}]$  to span space of all exponentials of the form  $\{e^{\Lambda_i^{e,e'} s} : \Lambda_{min}^{e,e'} \leq \Lambda_i^{e,e'} \leq \Lambda_{max}^{e,e'}\}$ .



# Mesh Independent Element Design Procedure

## Algorithm 1. "Build Your Own DEM Element"

Fix  $n^E \in \mathbb{N}$  (the desired number of angles defining  $\mathcal{V}^E$ ).

Select a set of  $n^E$  distinct angles  $\Theta^C = \{\theta_k\}_{k=1}^{n^E}$  between  $[0, 2\pi)$ .

Define the enrichment functions by:

$$c^E(\mathbf{x}; \Theta^C) = e^{\left(\frac{a_1 + |\mathbf{a}| \cos \Theta^C}{2\kappa}\right)(x - x_{r,i})} e^{\left(\frac{a_2 + |\mathbf{a}| \sin \Theta^C}{2\kappa}\right)(y - y_{r,i})}$$

Determine  $n^\lambda = \left\lfloor \frac{n^E}{4} \right\rfloor$ .

**for** each edge  $\Gamma^{e,e'} \in \Gamma^{\text{int}}$

Compute max and min of  $\frac{|\mathbf{a}|}{2\kappa} \left[ \cos(\phi - \alpha^{e,e'}) + \cos(\theta_k - \alpha^{e,e'}) \right]$ , call them  $\Lambda_{\min}^{e,e'}$ ,  $\Lambda_{\max}^{e,e'}$ .

Sample  $\{\Lambda_i^{e,e'} : i = 1, \dots, n^\lambda\}$  uniformly in the interval  $[\Lambda_{\min}^{e,e'}, \Lambda_{\max}^{e,e'}]$ .

Define the Lagrange multipliers approximations on  $\Gamma^{e,e'}$  by:

$$\lambda^h|_{\Gamma^{e,e'}} = \text{span} \left\{ e^{\Lambda_i^{e,e'}(s - s_{r,i}^{e,e'})}, 0 \leq s \leq h \right\}$$

**end for**



# Element Nomenclature

## Notation

DGM Element:  $Q - n^E - n^\lambda$

DEM Element:  $Q - n^E - n^{\lambda+} \equiv [Q - n^E - n^\lambda] \cup [Q_1]$

' $Q$ ': Quadrilateral

$n^E$ : Number of Enrichment Functions

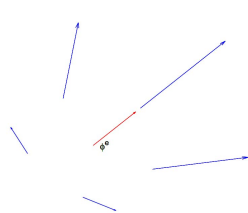
$n^\lambda$ : Number of Lagrange Multipliers per Edge

$Q_1$ : Galerkin Bilinear Quadrilateral Element

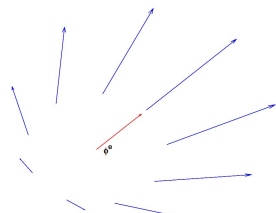
	Name	$n^E$	$\Theta^c$	$n^\lambda$
DGM elements	$Q - 4 - 1$	4	$\phi + \left\{ \frac{m\pi}{2} : m = 0, \dots, 3 \right\}$	1
	$Q - 8 - 2$	8	$\phi + \left\{ \frac{m\pi}{4} : m = 0, \dots, 7 \right\}$	2
	$Q - 12 - 3$	12	$\phi + \left\{ \frac{m\pi}{6} : m = 0, \dots, 11 \right\}$	3
	$Q - 16 - 4$	16	$\phi + \left\{ \frac{m\pi}{8} : m = 0, \dots, 15 \right\}$	4
DEM elements	$Q - 5 - 1^+$	5	$\phi + \left\{ \frac{2m\pi}{5} : m = 0, \dots, 4 \right\}$	1
	$Q - 9 - 2^+$	9	$\phi + \left\{ \frac{2m\pi}{9} : m = 0, \dots, 8 \right\}$	2
	$Q - 13 - 3^+$	13	$\phi + \left\{ \frac{2m\pi}{13} : m = 0, \dots, 12 \right\}$	3
	$Q - 17 - 4^+$	17	$\phi + \left\{ \frac{2m\pi}{17} : m = 0, \dots, 16 \right\}$	4



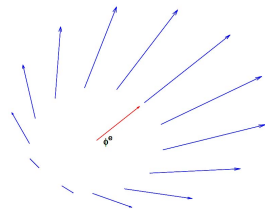
# Illustration of the Sets $\Theta^c$ for the True DEM Elements



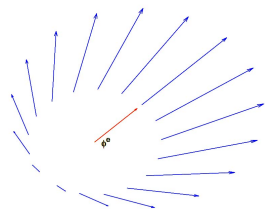
Q - 5 - 1<sup>+</sup>



Q - 9 - 2<sup>+</sup>



Q - 13 - 3<sup>+</sup>



Q - 17 - 4<sup>+</sup>



# Computational Complexities

Element	Asymptotic # of dofs	Stencil width for uniform $n \times n$ mesh	(# dofs) $\times$ (stencil width)	$L^2$ convergence rate ( <i>a posteriori</i> )
$Q_1$	$n_{el}$	9	$9n_{el}$	2
$Q - 4 - 1$	$2n_{el}$	7	$14n_{el}$	2
$Q_2$	$3n_{el}$	21	$63n_{el}$	3
$Q - 8 - 2$	$4n_{el}$	14	$56n_{el}$	3
$Q - 5 - 1^+$	$3n_{el}$	21	$63n_{el}$	2 - 3
$Q_3$	$5n_{el}$	33	$165n_{el}$	4
$Q - 12 - 3$	$6n_{el}$	21	$126n_{el}$	4
$Q - 9 - 2^+$	$5n_{el}$	33	$165n_{el}$	3 - 4
$Q_4$	$7n_{el}$	45	$315n_{el}$	5
$Q - 16 - 4$	$8n_{el}$	28	$224n_{el}$	5
$Q - 13 - 3^+$	$7n_{el}$	45	$315n_{el}$	4 - 5
$Q - 17 - 4^+$	$9n_{el}$	57	$513n_{el}$	4 - 5

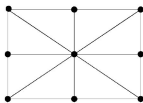


Figure 4:  $Q_1$  stencil

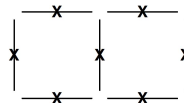


Figure 5:  $Q - 4 - 1$  stencil



# Summary of Computational Properties

## “COMPARABLES”

### *A priori* in computational cost:

- DGM with  $n$  LMs and  $Q_n$
- DEM with  $n$  LMs and  $Q_{n+1}$

### *A posteriori* in convergence rate:

- DGM with  $n$  LMs and  $Q_n$
- DEM with  $n$  LMs and  $Q_n/Q_{n+1}$

- Exponential enrichments  $\Rightarrow$  integrations can be computed analytically.
- $\mathcal{L}c^E = 0 \Rightarrow$  convert volume integrals to boundary integrals:

$$\begin{aligned} a(v^E, c^E) &= \int_{\hat{\Omega}} (\kappa \nabla v^E \cdot \nabla c^E + \mathbf{a} \cdot \nabla c^E v^E) d\Omega \\ &= \int_{\hat{\Gamma}} \nabla c^E \cdot \mathbf{n} v^E d\Gamma \end{aligned}$$



# Homogeneous Boundary Layer Problem

- $\Omega = (0, 1) \times (0, 1)$ ,  $f = 0$ .
- $\mathbf{a} = (\cos \phi, \sin \phi)$ .
- Dirichlet boundary conditions are specified on  $\Gamma$  such that the exact solution to the BVP is given by

$$c_{ex}(\mathbf{x}; \phi, \psi) = \frac{e^{\frac{1}{2\kappa} \{[\cos \phi + \cos \psi](x-1) + [\sin \phi + \sin \psi](y-1)\}} - 1}{e^{-\frac{1}{2\kappa} [\cos \phi + \cos \psi + \sin \phi + \sin \psi]} - 1}$$

- $\psi \in [0, 2\pi)$ : some flow direction (not necessarily aligned with  $\phi$ ).
- Solution exhibits a sharp exponential boundary layer in the advection direction  $\phi$ , whose gradient is a function of the Péclet number.

Figure 6:  $\phi = \psi = 0$

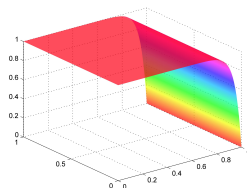
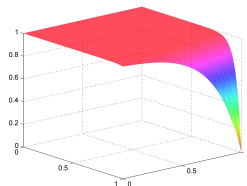


Figure 7:  $\phi = \pi/7, \psi = 0$



# Homogeneous Boundary Layer Problem

- $\Omega = (0, 1) \times (0, 1)$ ,  $f = 0$ .
- $\mathbf{a} = (\cos \phi, \sin \phi)$ .
- Dirichlet boundary conditions are specified on  $\Gamma$  such that the exact solution to the BVP is given by

$$c_{ex}(\mathbf{x}; \phi, \psi) = \frac{e^{\frac{1}{2\kappa} \{[\cos \phi + \cos \psi](x-1) + [\sin \phi + \sin \psi](y-1)\}} - 1}{e^{-\frac{1}{2\kappa} [\cos \phi + \cos \psi + \sin \phi + \sin \psi]} - 1}$$

- $\psi \in [0, 2\pi)$ : some flow direction (not necessarily aligned with  $\phi$ ).
- Solution exhibits a sharp exponential boundary layer in the advection direction  $\phi$ , whose gradient is a function of the Péclet number.

Homogeneous problem  $\Rightarrow$   
pure DGM elements sufficient

Figure 6:  $\phi = \psi = 0$

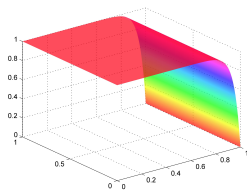
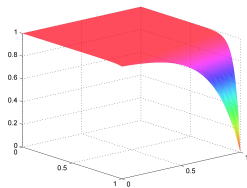


Figure 7:  $\phi = \pi/7, \psi = 0$



# Non-trivial Test Case: Flow *not* Aligned with Advection Direction ( $\phi \neq \psi$ )

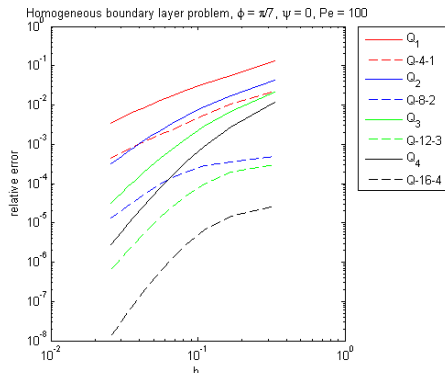
- Set  $\phi = \pi/7$ ; vary  $\psi$ .
- Can show that  $c_{ex} \notin \mathcal{V}^E$  for any DGM elements and advection directions tested here.

**Table 1:** Relative  $L^2(\Omega)$  errors,  $\approx 1600$  dofs, unstructured mesh,  $\phi = \pi/7$ ,  $Pe = 10^3$ : Galerkin vs. DGM elts.

$\psi/\pi$	$Q_1$	$Q - 4 - 1$	$Q_2$	$Q - 8 - 2$
0	$1.45 \times 10^{-2}$	$1.65 \times 10^{-3}$	$5.92 \times 10^{-3}$	$1.79 \times 10^{-3}$
1/4	$1.52 \times 10^{-2}$	$9.38 \times 10^{-4}$	$6.06 \times 10^{-3}$	$2.54 \times 10^{-4}$
1/2	$1.51 \times 10^{-2}$	$9.23 \times 10^{-4}$	$5.97 \times 10^{-3}$	$2.12 \times 10^{-4}$
$\psi/\pi$	$Q_3$	$Q - 12 - 3$	$Q_4$	$Q - 16 - 4$
0	$4.34 \times 10^{-3}$	$1.10 \times 10^{-4}$	$3.23 \times 10^{-3}$	$2.30 \times 10^{-5}$
1/4	$4.46 \times 10^{-3}$	$1.23 \times 10^{-5}$	$3.29 \times 10^{-3}$	$8.82 \times 10^{-7}$
1/2	$4.36 \times 10^{-3}$	$1.11 \times 10^{-5}$	$3.18 \times 10^{-3}$	$1.59 \times 10^{-6}$



# Convergence Analysis & Results



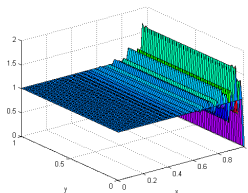
Element	Rate of convergence	# dofs to achieve $10^{-3}$ error
$Q_1$	1.90	63,266
$Q-4-1$	1.99	14,320
$Q_2$	2.38	24,300
$Q-8-2$	3.27	5400
$Q_3$	3.48	12,500
$Q-12-3$	3.88	850
$Q_4$	4.41	8600
$Q-16-4$	5.19	570

- To achieve for this problem the relative error of 0.1% for  $Pe = 10^3$ :
  - $Q-4-1$  requires 4.4 times fewer dofs than  $Q_1$ .
  - $Q-8-2$  requires 4.5 times fewer dofs than  $Q_2$ .
  - $Q-12-3$  requires 14.7 times fewer dofs than  $Q_3$ .
  - $Q-16-4$  requires 15.1 times fewer dofs than  $Q_4$ .

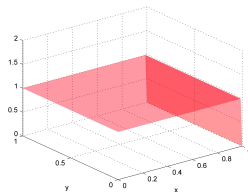


# Solution Plots for Homogeneous BVP

Figure 8:  $\phi = \psi = 0$ ,  $Pe = 10^3$ ,  $\approx 1600$  dofs

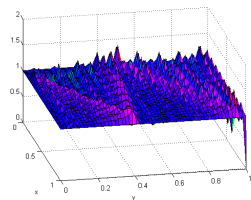


$Q_3$

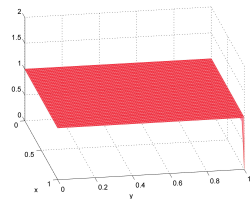


$Q - 12 - 3$

Figure 9:  $\phi = \pi/7$ ,  $\psi = 0$ ,  $Pe = 10^5$ ,  $\approx 1600$  dofs



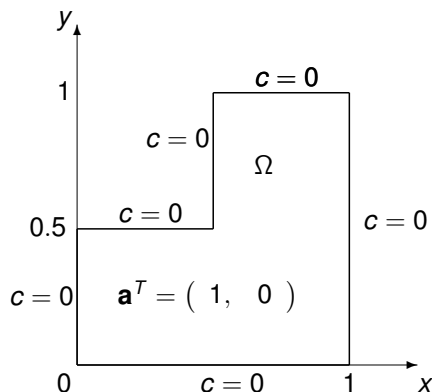
$Q_3$



$Q - 12 - 3$



# Double Ramp Problem on an $L$ -Shaped Domain



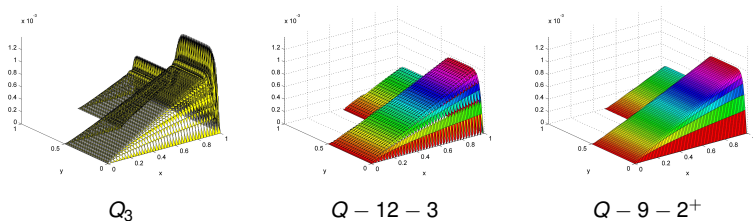
- Homogeneous Dirichlet boundary conditions are prescribed on all six sides of  $L$ -shaped domain  $\Omega$ .
- Advection direction:  $\phi = 0$ .
- Source:  $f = 1$ .
- Strong outflow boundary layer along the line  $x = 1$ .
- Two crosswind boundary layers along  $y = 0$  and  $y = 1$ .
- A crosswind internal layer along  $y = 0.5$ .

Figure 10:  $L$ -shaped domain for double ramp problem



# Solutions Plots: Galerkin vs. DGM vs. DEM Elements

Figure 11:  $L$ -shaped double ramp problem solutions:  $Pe = 10^3$ , 7600 dofs

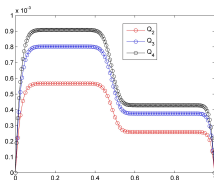


- No oscillations can be seen in the computed DGM and DEM solutions.
- Would expect: DEM elements to outperform DGM elements for this *inhomogeneous* problem.
- In fact: DGM elements experience some difficulty along the  $y = 0.5$  line, the location of the crosswind internal layer.

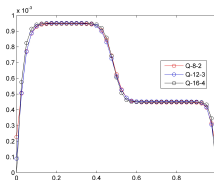


# Cross Sectional Solution Plots

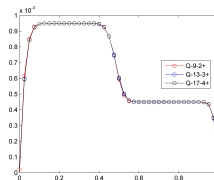
Figure 12: Solution along the line  $x = 0.9$  with 7600 dofs



Galerkin

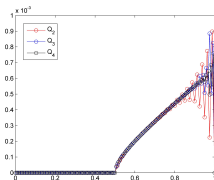


DGM

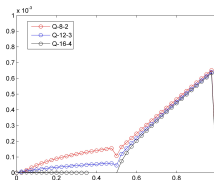


DEM

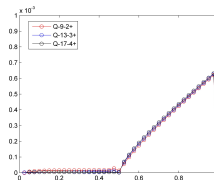
Figure 13: Solution along the line  $y = 0.5$  with 7600 dofs



Galerkin



DGM



DEM



Relative Errors ( $Pe = 10^3$ , Uniform Mesh)

# elements	$Q_3$	$Q - 12 - 3$	$Q - 9 - 2^+$
300	$1.49 \times 10^{-1}$	$1.11 \times 10^{-1}$	$4.11 \times 10^{-2}$
1200	$6.57 \times 10^{-2}$	$5.00 \times 10^{-2}$	$8.47 \times 10^{-3}$
4800	$2.36 \times 10^{-2}$	$1.02 \times 10^{-2}$	$1.65 \times 10^{-3}$
10,800	$1.08 \times 10^{-2}$	$4.54 \times 10^{-3}$	$7.43 \times 10^{-4}$
# elements	$Q_4$	$Q - 16 - 4$	$Q - 13 - 3^+$
300	$9.58 \times 10^{-2}$	$8.32 \times 10^{-2}$	$2.80 \times 10^{-2}$
1200	$3.78 \times 10^{-2}$	$1.33 \times 10^{-2}$	$4.71 \times 10^{-3}$
4800	$1.03 \times 10^{-2}$	$9.17 \times 10^{-3}$	$8.24 \times 10^{-4}$
10,800	$3.70 \times 10^{-3}$	$4.92 \times 10^{-4}$	$9.75 \times 10^{-5}$

- DEM elements outperform DGM elements.
- Both DGM and DEM elements outperform Galerkin elements.



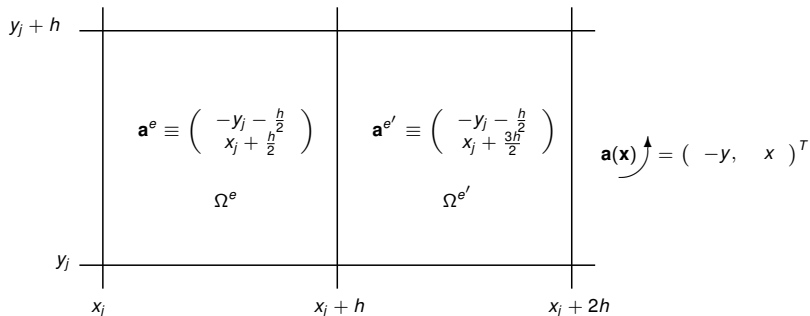
# Outline

- 1 Motivation
- 2 Advection-Diffusion Equation
- 3 Discontinuous Enrichment Method (DEM)
- 4 DEM for Constant-Coefficient Advection-Diffusion
  - Enrichment Bases
  - Lagrange Multiplier Approximations
  - Element Design
  - Numerical Experiments
- 5 DEM for Variable-Coefficient Advection-Diffusion
  - Enrichment Bases
  - Lagrange Multiplier Approximations
  - Element Design
  - Numerical Experiments
- 6 Extension of DEM to Unsteady, Non-Linear Problems
- 7 Summary



# Extension to Variable-Coefficient Problems

- Define  $\mathcal{V}^E$  within each element as the free-space solutions to the homogeneous PDE, with locally-frozen coefficients.
- $\mathbf{a}(\mathbf{x}) \approx \mathbf{a}^e = \text{constant}$  inside each element  $\Omega^e$  as  $h \rightarrow 0$ :  
 $\{\mathbf{a}(\mathbf{x}) \cdot \nabla c - \kappa \Delta c = f(\mathbf{x}) \text{ in } \Omega\} \approx \cup_{e=1}^{n_{el}} \{\mathbf{a}^e \cdot \nabla c - \kappa \Delta c = f(\mathbf{x}) \text{ in } \Omega^e\}$ .



- Enrichment in each element:

$$c_e^E(\mathbf{x}; \theta_i^e) = e^{\frac{|\mathbf{a}^e|}{2\kappa} (\cos \phi^e + \cos \theta_i^e)(x - x_{r,i}^e)} e^{\frac{|\mathbf{a}^e|}{2\kappa} (\sin \phi^e + \sin \theta_i^e)(y - y_{r,i}^e)} \in \mathcal{V}_e^E$$



# Relation Between Local Enrichment and Governing PDE

- Given  $\mathbf{a}(\mathbf{x}) \in C^1(\Omega^e)$ , Taylor expand  $\mathbf{a}(\mathbf{x})$  around an element's midpoint  $\bar{\mathbf{x}}^e$ :

$$\mathbf{a}(\mathbf{x}) = \mathbf{a}(\bar{\mathbf{x}}^e) + \nabla \mathbf{a}|_{\mathbf{x}=\bar{\mathbf{x}}^e} \cdot (\mathbf{x} - \bar{\mathbf{x}}^e) + \mathcal{O}(\mathbf{x} - \bar{\mathbf{x}}^e)^2 \quad \text{in } \Omega^e$$



# Relation Between Local Enrichment and Governing PDE

- Given  $\mathbf{a}(\mathbf{x}) \in C^1(\Omega^e)$ , Taylor expand  $\mathbf{a}(\mathbf{x})$  around an element's midpoint  $\bar{\mathbf{x}}^e$ :

$$\mathbf{a}(\mathbf{x}) = \mathbf{a}(\bar{\mathbf{x}}^e) + \nabla \mathbf{a}|_{\mathbf{x}=\bar{\mathbf{x}}^e} \cdot (\mathbf{x} - \bar{\mathbf{x}}^e) + \mathcal{O}(\mathbf{x} - \bar{\mathbf{x}}^e)^2 \quad \text{in } \Omega^e$$

- Operator governing the PDE inside the element  $\Omega^e$  takes the form

$$\mathbf{a}(\mathbf{x}) \cdot \nabla c - \kappa \Delta c = \mathcal{L}_e c + f(c) \quad \text{in } \Omega^e$$

where

$$\mathcal{L}_e c \equiv \mathbf{a}(\bar{\mathbf{x}}^e) \cdot \nabla c - \kappa \Delta c$$

$$f(c) \equiv [\nabla \mathbf{a}|_{\mathbf{x}=\bar{\mathbf{x}}^e} \cdot (\mathbf{x} - \bar{\mathbf{x}}^e) + \mathcal{O}(\mathbf{x} - \bar{\mathbf{x}}^e)^2] \cdot \nabla c$$



# Relation Between Local Enrichment and Governing PDE

- Given  $\mathbf{a}(\mathbf{x}) \in C^1(\Omega^e)$ , Taylor expand  $\mathbf{a}(\mathbf{x})$  around an element's midpoint  $\bar{\mathbf{x}}^e$ :

$$\mathbf{a}(\mathbf{x}) = \mathbf{a}(\bar{\mathbf{x}}^e) + \nabla \mathbf{a}|_{\mathbf{x}=\bar{\mathbf{x}}^e} \cdot (\mathbf{x} - \bar{\mathbf{x}}^e) + \mathcal{O}(\mathbf{x} - \bar{\mathbf{x}}^e)^2 \quad \text{in } \Omega^e$$

- Operator governing the PDE inside the element  $\Omega^e$  takes the form

$$\mathbf{a}(\mathbf{x}) \cdot \nabla c - \kappa \Delta c = \mathcal{L}_e c + f(c) \quad \text{in } \Omega^e$$

where

$$\mathcal{L}_e c \equiv \mathbf{a}(\bar{\mathbf{x}}^e) \cdot \nabla c - \kappa \Delta c$$

$$f(c) \equiv [\nabla \mathbf{a}|_{\mathbf{x}=\bar{\mathbf{x}}^e} \cdot (\mathbf{x} - \bar{\mathbf{x}}^e) + \mathcal{O}(\mathbf{x} - \bar{\mathbf{x}}^e)^2] \cdot \nabla c$$

- “Residual” advection equation acts as source-like term  $\Rightarrow$  suggests true DEM elements are in general more appropriate than pure DGM elements for variable-coefficient problems.



# Relation Between Local Enrichment and Governing PDE

- Given  $\mathbf{a}(\mathbf{x}) \in C^1(\Omega^e)$ , Taylor expand  $\mathbf{a}(\mathbf{x})$  around an element's midpoint  $\bar{\mathbf{x}}^e$ :

$$\mathbf{a}(\mathbf{x}) = \mathbf{a}(\bar{\mathbf{x}}^e) + \nabla \mathbf{a}|_{\mathbf{x}=\bar{\mathbf{x}}^e} \cdot (\mathbf{x} - \bar{\mathbf{x}}^e) + \mathcal{O}(\mathbf{x} - \bar{\mathbf{x}}^e)^2 \quad \text{in } \Omega^e$$

- Operator governing the PDE inside the element  $\Omega^e$  takes the form

$$\mathbf{a}(\mathbf{x}) \cdot \nabla c - \kappa \Delta c = \mathcal{L}_e c + f(c) \quad \text{in } \Omega^e$$

where

$$\mathcal{L}_e c \equiv \mathbf{a}(\bar{\mathbf{x}}^e) \cdot \nabla c - \kappa \Delta c$$

$$f(c) \equiv [\nabla \mathbf{a}|_{\mathbf{x}=\bar{\mathbf{x}}^e} \cdot (\mathbf{x} - \bar{\mathbf{x}}^e) + \mathcal{O}(\mathbf{x} - \bar{\mathbf{x}}^e)^2] \cdot \nabla c$$

- "Residual" advection equation acts as source-like term  $\Rightarrow$  suggests true DEM elements are in general more appropriate than pure DGM elements for variable-coefficient problems.

Can we build a better **pure DGM** element for variable-coefficient problems?



# Additional “First Order” Enrichment Functions

- Are we missing any free-space solutions to  $\mathbf{a}^e \cdot \nabla c^E - \kappa \Delta c^E = 0$ ?



# Additional “First Order” Enrichment Functions

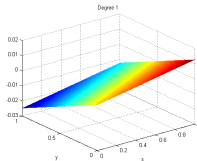
- Are we missing any free-space solutions to  $\mathbf{a}^e \cdot \nabla c^E - \kappa \Delta c^E = 0$ ?
- Yes! Polynomial free-space solutions to  $\mathcal{L}c_{e,n}^E = \mathbf{a}^e \cdot \nabla c_{e,n}^E - \Delta c_{e,n}^E = 0$  (of any desired degree  $n$ ) can be derived as well.



# Additional “First Order” Enrichment Functions

- Are we missing any free-space solutions to  $\mathbf{a}^e \cdot \nabla c^E - \kappa \Delta c^E = 0$ ?
- Yes! Polynomial free-space solutions to  $\mathcal{L}c_{e,n}^E = \mathbf{a}^e \cdot \nabla c_{e,n}^E - \Delta c_{e,n}^E = 0$  (of any desired degree  $n$ ) can be derived as well.

$$c_{e,1}^E(\mathbf{x}) = |\mathbf{a}^e \times \mathbf{x}|$$



$$c_{e,1}^E(\mathbf{x})$$

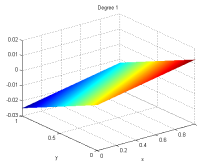
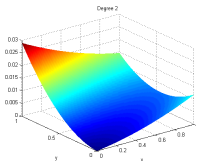


# Additional “First Order” Enrichment Functions

- Are we missing any free-space solutions to  $\mathbf{a}^e \cdot \nabla c^E - \kappa \Delta c^E = 0$ ?
- Yes! Polynomial free-space solutions to  $\mathcal{L}c_{e,n}^E = \mathbf{a}^e \cdot \nabla c_{e,n}^E - \Delta c_{e,n}^E = 0$  (of any desired degree  $n$ ) can be derived as well.

$$c_{e,1}^E(\mathbf{x}) = |\mathbf{a}^e \times \mathbf{x}|$$

$$c_{e,2}^E(\mathbf{x}) = |\mathbf{a}^e \times \mathbf{x}|^2 + 2(\mathbf{a}^e \cdot \mathbf{x})$$


 $c_{e,1}^E(\mathbf{x})$ 

 $c_{e,2}^E(\mathbf{x})$ 

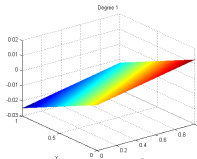
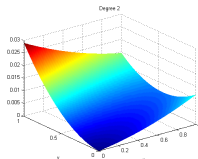
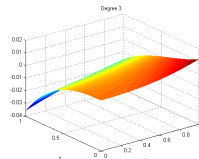

# Additional “First Order” Enrichment Functions

- Are we missing any free-space solutions to  $\mathbf{a}^e \cdot \nabla c^E - \kappa \Delta c^E = 0$ ?
- Yes! Polynomial free-space solutions to  $\mathcal{L}c_{e,n}^E = \mathbf{a}^e \cdot \nabla c_{e,n}^E - \Delta c_{e,n}^E = 0$  (of any desired degree  $n$ ) can be derived as well.

$$c_{e,1}^E(\mathbf{x}) = |\mathbf{a}^e \times \mathbf{x}|$$

$$c_{e,2}^E(\mathbf{x}) = |\mathbf{a}^e \times \mathbf{x}|^2 + 2(\mathbf{a}^e \cdot \mathbf{x})$$

$$c_{e,3}^E(\mathbf{x}) = |\mathbf{a}^e \times \mathbf{x}|^3 + 6|\mathbf{a}^e \times \mathbf{x}|(\mathbf{a}^e \cdot \mathbf{x})$$

$$\vdots$$

 $c_{e,1}^E(\mathbf{x})$ 

 $c_{e,2}^E(\mathbf{x})$ 

 $c_{e,3}^E(\mathbf{x})$ 


# “Higher Order” Enrichment Functions

- Linearize  $\mathbf{a}(\mathbf{x})$  to second order, instead of to first order:

$$\mathbf{a}(\mathbf{x}) \approx \mathbf{a}(\bar{\mathbf{x}}^e) + \nabla \mathbf{a}|_{\mathbf{x}=\bar{\mathbf{x}}^e} \cdot (\mathbf{x} - \bar{\mathbf{x}}^e) \quad \text{in } \Omega^e$$

- Enrich with free-space solutions to

$$[\mathbf{A}\mathbf{x} + \mathbf{b}] \cdot \nabla c^E - \kappa \Delta c^E = 0 \quad (2)$$

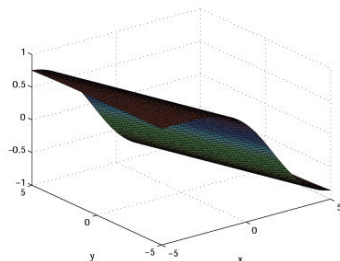
where  $\mathbf{A} \equiv \nabla \mathbf{a}|_{\mathbf{x}=\bar{\mathbf{x}}^e}$ ,  $\mathbf{b} \equiv (\mathbf{a}(\bar{\mathbf{x}}^e) - \nabla \mathbf{a}|_{\mathbf{x}=\bar{\mathbf{x}}^e} \bar{\mathbf{x}}^e)$ .

- Solutions to (2) are given by:

$$c^E(\mathbf{x}) = \int_0^{\mathbf{v}_i \cdot \mathbf{x}} \exp \left\{ \frac{\sigma_i w^2}{2} + (\mathbf{v}_i \cdot \mathbf{b}) w \right\} dw$$

$\sigma_i =$  eigenvalue of  $\nabla \mathbf{a}|_{\mathbf{x}=\bar{\mathbf{x}}^e}$

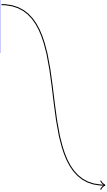
$\mathbf{v}_i =$  eigenvector of  $\nabla \mathbf{a}|_{\mathbf{x}=\bar{\mathbf{x}}^e}$



# “Enrichment Function Bank”

## Exponential Family

$$c_e^E(\mathbf{x}; \theta_i) = e^{\left(\frac{a_1^e + |a^e| \cos \theta_i}{2\kappa}\right)(x - x_{r,i})} e^{\left(\frac{a_2^e + |a^e| \sin \theta_i}{2\kappa}\right)(y - y_{r,i})}$$



$\mathcal{V}_e^E$



# “Enrichment Function Bank”

## Exponential Family

$$c_e^E(\mathbf{x}; \theta_i) = e^{\left(\frac{a_1^e + |\mathbf{a}^e| \cos \theta_i}{2\kappa}\right)(x - x_{r,i})} e^{\left(\frac{a_2^e + |\mathbf{a}^e| \sin \theta_i}{2\kappa}\right)(y - y_{r,i})}$$

## Polynomial Family

$$c_{e,0}^E(\mathbf{x}) = 1$$

$$c_{e,1}^E(\mathbf{x}) = |\mathbf{a}^e \times \mathbf{x}|$$

$$c_{e,2}^E(\mathbf{x}) = |\mathbf{a}^e \times \mathbf{x}|^2 + 2(\mathbf{a}^e \cdot \mathbf{x})$$

$$c_{e,3}^E(\mathbf{x}) = |\mathbf{a}^e \times \mathbf{x}|^3 + 6|\mathbf{a}^e \times \mathbf{x}|(\mathbf{a}^e \cdot \mathbf{x})$$

$$\vdots$$

$$\mathcal{V}_e^E$$


# “Enrichment Function Bank”

## Exponential Family

$$c_e^E(\mathbf{x}; \theta_i) = e^{\left(\frac{a_1^e + |a^e| \cos \theta_i}{2\kappa}\right)(x - x_{r,i})} e^{\left(\frac{a_2^e + |a^e| \sin \theta_i}{2\kappa}\right)(y - y_{r,i})}$$

## Polynomial Family

$$c_{e,0}^E(\mathbf{x}) = 1$$

$$c_{e,1}^E(\mathbf{x}) = |a^e \times \mathbf{x}|$$

$$c_{e,2}^E(\mathbf{x}) = |a^e \times \mathbf{x}|^2 + 2(a^e \cdot \mathbf{x})$$

$$c_{e,3}^E(\mathbf{x}) = |a^e \times \mathbf{x}|^3 + 6|a^e \times \mathbf{x}|(a^e \cdot \mathbf{x})$$

$$\vdots$$

## “Higher Order” Enrichment

$$c^E(\mathbf{x}) = \int_0^{\mathbf{v}_i \cdot \mathbf{x}} \exp\left\{\frac{\sigma_i w^2}{2} + (\mathbf{v}_i \cdot \mathbf{b})w\right\} dw$$

$$\mathcal{V}_e^E$$


# Modification of the Lagrange Multiplier Field

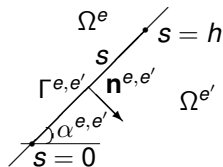


Figure 14: Straight edge  $\Gamma^{e,e'}$  oriented at angle  $\alpha^{e,e'} \in [0, 2\pi)$

Limit  $n^\lambda$  to satisfy *inf-sup*:  
 Use  $\left\{ \begin{array}{l} \left[ \frac{n^{\text{exp}}}{4} \right] \text{ exponential LMs} \\ \left[ \frac{n^{\text{pol}}}{4} \right] \text{ polynomial LMs} \end{array} \right.$

- LM approximations arising from exponential enrichments:

$$\lambda^h|_{\Gamma^{e,e'}} = \text{span} \left\{ e^{\Lambda_i^{e,e'}(s-s_{r,i}^{e,e'})}, 0 \leq s \leq h, 1 \leq i \leq n^{\text{exp}} \right\}$$

where  $\Lambda_i^{e,e'} \equiv \frac{|a|}{2\kappa} \left[ \cos(\phi - \alpha^{e,e'}) + \cos(\theta_i - \alpha^{e,e'}) \right]$ .

- LM approximations arising from polynomial enrichments:

$$\lambda^h|_{\Gamma^{e,e'}} = \text{span} \left\{ s^k, 0 \leq s \leq h, 0 \leq k \leq n^{\text{pol}} - 1 \right\}$$



# New DGM Elements

## Notation

$$\text{New DGM Elements: } \begin{cases} Q - (n^{\text{pol}}, n^{\text{exp}}) - n^\lambda \\ Q - (n^{\text{pol}}, n^{\text{exp}})^* - n^\lambda \end{cases}$$

' $Q$ ': Quadrilateral

$n^{\text{pol}}$ : Number of Polynomial Enrichment Functions

$n^{\text{exp}}$ : Number of Exponential Enrichment Functions

$n^\lambda$ : Number of Lagrange Multipliers per Edge

'\*': Element Augmented by "Higher Order" Enrichment

	Name	$n^E$	$\Theta^c$	$n^\lambda$
DGM elements	$Q - (4, 5) - 2$	9	$\phi + \left\{ \frac{2m\pi}{5} : m = 0, \dots, 4 \right\}$	2
	$Q - (4, 5)^* - 2$	10	$\phi + \left\{ \frac{2m\pi}{5} : m = 0, \dots, 4 \right\}$	2
	$Q - (4, 9) - 3$	13	$\phi + \left\{ \frac{2m\pi}{9} : m = 0, \dots, 8 \right\}$	3
	$Q - (4, 9)^* - 3$	14	$\phi + \left\{ \frac{2m\pi}{9} : m = 0, \dots, 8 \right\}$	3

- Polynomial enrichment fields of new DGM elements contain  $n^{\text{pol}} = 4$  polynomial free-space solutions of degrees 0, 1, 2 and 3.

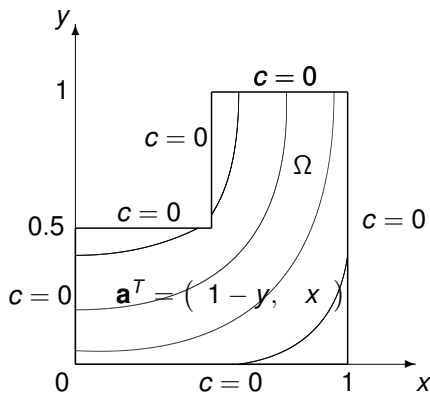


# Computational Complexities

Element	Asymptotic # of dofs	Stencil width for uniform $n \times n$ mesh	(# dofs) $\times$ (stencil width)	$L^2$ convergence rate ( <i>a posteriori</i> )
$Q_1$	$n_{el}$	9	$9n_{el}$	2
$Q - 4 - 1$	$2n_{el}$	7	$14n_{el}$	2
$Q_2$	$3n_{el}$	21	$63n_{el}$	3
$Q - 8 - 2$	$4n_{el}$	14	$56n_{el}$	3
$Q - (4, 5) - 2$	$4n_{el}$	14	$63n_{el}$	3
$Q - (4, 5)^* - 2$	$4n_{el}$	14	$63n_{el}$	3
$Q - 5 - 1^+$	$3n_{el}$	21	$63n_{el}$	2 - 3
$Q_3$	$5n_{el}$	33	$165n_{el}$	4
$Q - 12 - 3$	$6n_{el}$	21	$126n_{el}$	4
$Q - (4, 9) - 3$	$6n_{el}$	21	$126n_{el}$	4
$Q - (4, 9)^* - 3$	$6n_{el}$	21	$126n_{el}$	4
$Q - 9 - 2^+$	$5n_{el}$	33	$165n_{el}$	3 - 4
$Q_4$	$7n_{el}$	45	$315n_{el}$	5
$Q - 16 - 4$	$8n_{el}$	28	$224n_{el}$	5
$Q - 13 - 3^+$	$7n_{el}$	45	$315n_{el}$	4 - 5
$Q - 17 - 4^+$	$9n_{el}$	57	$513n_{el}$	4 - 5



# Inhomogeneous Rotating Advection Problem on an $L$ -Shaped Domain

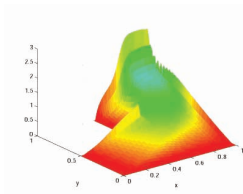
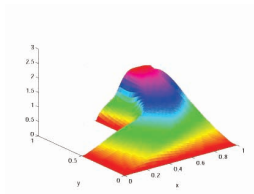
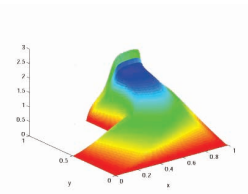
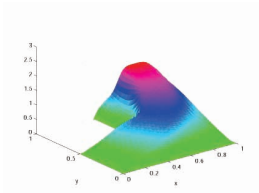
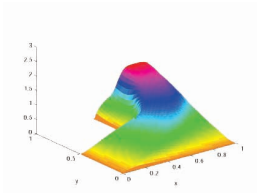


**Figure 15:**  $L$ -shaped domain and rotating velocity field (curved lines indicate streamlines)

- Homogeneous Dirichlet boundary conditions are prescribed on all six sides of  $L$ -shaped domain  $\Omega$ .
- Source:  $f = 1$ .
- $\mathbf{a}^T(\mathbf{x}) = (1 - y, x)$ .
- Outflow boundary layer along the line  $y = 1$ .
- Second boundary layer that terminates in the vicinity of the re-entrant corner  $(x, y) = (0.5, 0.5)$ .



# Solutions Plots for $Pe = 10^3$ with $\approx 3000$ dofs

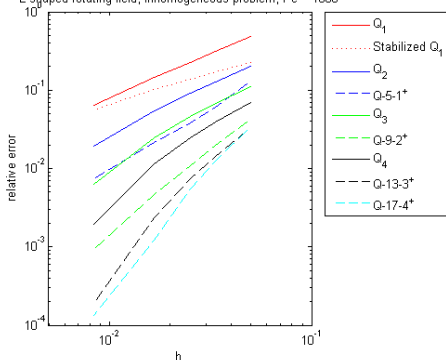

 $Q_1$ 

 Stabilized  $Q_1$ 

 $Q_2$ 

 $Q - 5 - 1^+$ 

 $Q - 9 - 2^+$ 

\* "Stabilized  $Q_1$ " is upwind stabilized bilinear finite element proposed by Harari *et al.*



# Convergence Analysis & Results

L-shaped rotating field, inhomogeneous problem,  $Pe = 1000$



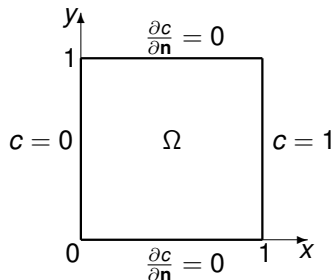
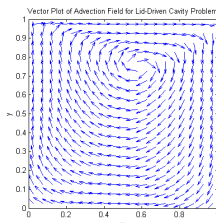
Element	Rate of convergence	# dofs to achieve $10^{-2}$ error
$Q_2$	1.94	62,721
$Q - 5 - 1^+$	1.55	21,834
$Q_3$	2.67	33,707
$Q - 9 - 2^+$	2.37	7,568
$Q_4$	3.50	20,796
$Q - 13 - 3^+$	3.23	5,935
$Q - 17 - 4^+$	3.26	4,802

\* "Stabilized  $Q_1$ " is upwind stabilized bilinear finite element proposed by Harari *et al.*

- To achieve for this problem the relative error of 1% for  $Pe = 10^3$ :
  - $Q - 5 - 1^+$  requires 2.9 times fewer dofs than  $Q_2$ .
  - $Q - 9 - 2^+$  requires 4.5 times fewer dofs than  $Q_3$ .
  - $Q - 13 - 3^+$  requires 3.5 times fewer dofs than  $Q_4$ .



# Lid-Driven Cavity Flow Problem

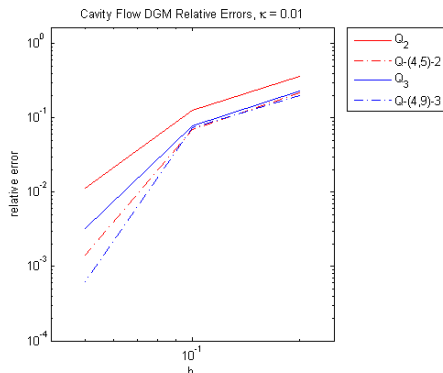


- $\Omega = (0, 1) \times (0, 1)$ ,  $f = 0$ .
- $\mathbf{a}(\mathbf{x})$  computed numerically by solving the incompressible Navier-Stokes equations for lid-driven cavity flow problem (stationary sides and bottom, tangential movement of top).
- Advection field reconstructed using interpolation with bilinear shape functions  $\phi_i^e$ :

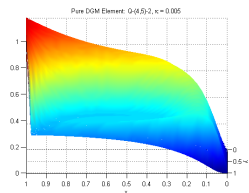
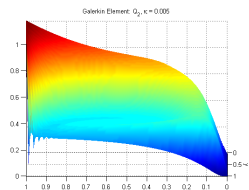
$$\mathbf{a}^e(\boldsymbol{\xi}) = \sum_{i=1}^{\# \text{ nodes of } \Omega^e} \mathbf{a}_i^e \phi_i^e(\boldsymbol{\xi})$$

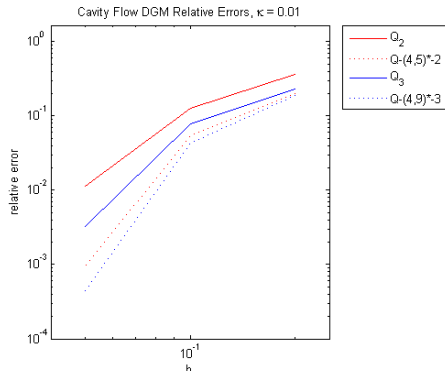
- $c(\mathbf{x})$  represents temperature in cavity.



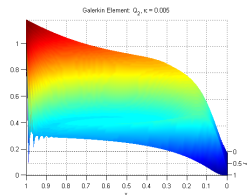
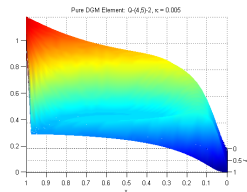
Convergence Analysis & Results ( $\kappa = 0.01$ ,  $Pe \approx 260$ )

- New pure DGM elements without “higher order” enrichment outperform Galerkin comparables.



Convergence Analysis & Results ( $\kappa = 0.01$ ,  $Pe \approx 260$ )

- New pure DGM elements without “higher order” enrichment outperform Galerkin comparables.
- Further improvement in computation by adding “higher order” enrichment.

 $Q_2$  $Q - (4, 5) - 2$ 

# Outline

- 1 Motivation
- 2 Advection-Diffusion Equation
- 3 Discontinuous Enrichment Method (DEM)
- 4 DEM for Constant-Coefficient Advection-Diffusion
  - Enrichment Bases
  - Lagrange Multiplier Approximations
  - Element Design
  - Numerical Experiments
- 5 DEM for Variable-Coefficient Advection-Diffusion
  - Enrichment Bases
  - Lagrange Multiplier Approximations
  - Element Design
  - Numerical Experiments
- 6 Extension of DEM to Unsteady, Non-Linear Problems
- 7 Summary



# DEM for the Viscous Burgers Equation

- Non-linear unsteady version of advection-diffusion equation = **viscous Burgers equation**:

$$u_t + uu_x - \kappa u_{xx} = 0$$



# DEM for the Viscous Burgers Equation

- Non-linear unsteady version of advection-diffusion equation = **viscous Burgers equation**:

$$u_t + uu_x - \kappa u_{xx} = 0$$

- Semi-discrete form of PDE (with semi-implicit Euler) at time  $n$ :

$$\frac{u^{n+1} - u^n}{\Delta t} + u^n u_x^{n+1} - \kappa u_{xx}^{n+1} = 0$$



# DEM for the Viscous Burgers Equation

- Non-linear unsteady version of advection-diffusion equation = **viscous Burgers equation**:

$$u_t + uu_x - \kappa u_{xx} = 0$$

- Semi-discrete form of PDE (with semi-implicit Euler) at time  $n$ :

$$\frac{u^{n+1} - u^n}{\Delta t} + u^n u_x^{n+1} - \kappa u_{xx}^{n+1} = 0$$

- Enrichment functions inside each element at time step  $n$  are the free-space solutions to steady version of the equation above:

$$\mathcal{V}_e^{E,n} = \text{span}\{u^n(x) : u^{n-1}(\bar{x}_e)u_x^n - \kappa u_{xx}^n = 0, x \in \Omega^e\}$$

where

$\mathcal{V}_e^{E,n}$  = enrichment field inside element  $\Omega^e$  at time step  $n$

$\bar{x}_e \equiv$  midpoint of element  $\Omega^e$



# Outline

- 1 Motivation
- 2 Advection-Diffusion Equation
- 3 Discontinuous Enrichment Method (DEM)
- 4 DEM for Constant-Coefficient Advection-Diffusion
  - Enrichment Bases
  - Lagrange Multiplier Approximations
  - Element Design
  - Numerical Experiments
- 5 DEM for Variable-Coefficient Advection-Diffusion
  - Enrichment Bases
  - Lagrange Multiplier Approximations
  - Element Design
  - Numerical Experiments
- 6 Extension of DEM to Unsteady, Non-Linear Problems
- 7 Summary



# Summary

**Discontinuous Enrichment Method (DEM)** = efficient, competitive alternative to stabilized FEMs for advection-diffusion in a high Péclet regime.

- Parametrization of exponential basis enables systematic design of DEM elements of arbitrary orders.
- Augmentation of enrichment space with additional free-space solutions can improve further the approximation.
- For all test problems, enriched elements outperform their Galerkin and stabilized Galerkin counterparts of comparable computational complexity, sometimes by many orders of magnitude.
- In a high Péclet regime, DGM and DEM solutions are almost completely oscillation-free, in contrast with the Galerkin solutions.
- Advection-diffusion work generalizable to more complex equations in fluid mechanics (e.g., non-linear, unsteady, 3D).
- Future work: DEM for incompressible Navier-Stokes.



# References

([www.stanford.edu/~irinak/pubs.html](http://www.stanford.edu/~irinak/pubs.html))

- [1] **I. Kalashnikova**, R. Tezaur, C. Farhat. A Discontinuous Enrichment Method for Variable Coefficient Advection-Diffusion at High Peclet Number. *Int. J. Numer. Meth. Engng.* (accepted)
- [2] C. Farhat, **I. Kalashnikova**, R. Tezaur. A Higher-Order Discontinuous Enrichment Method for the Solution of High Peclet Advection-Diffusion Problems on Unstructured Meshes. *Int. J. Numer. Meth. Engng.* **81** (2010) 604-636.
- [3] **I. Kalashnikova**, C. Farhat, R. Tezaur. A Discontinuous Enrichment Method for the Solution of Advection-Diffusion Problems in high Peclet Number Regimes. *Fin. El. Anal. Des.* **45** (2009) 238-250.
- [4] R. Tezaur, C. Farhat. Three-dimensional discontinuous Galerkin elements with plane waves and Lagrange multipliers for the solution of mid-frequency Helmholtz problems. *Int. J. Numer. Methods Engng.* **66** (2006) 796-815.
- [5] C. Farhat, R. Tezaur, J. Toivanen. A domain decomposition method for discontinuous Galerkin discretization of Helmholtz problems with plane waves and Lagrange multipliers. *Int. J. Numer. Method. Engng.* **78** (2009) 1513-1531.
- [6] R. Tezaur, L. Zhang, C. Farhat. A discontinuous method for capturing evanescent waves in multi-scale fluid and fluid/solid problems. *Comput. Methods Appl. Mech. Engng.* **197** (2008) 1680-1698.
- [7] P. Massimi, R. Tezaur, C. Farhat. A discontinuous enrichment method for three-dimensional multiscale harmonic wave propagation problems in multi-fluid and fluid-solid media. *Int. J. Numer. Methods Engng.* **76** (2008) 400-425.
- [8] L. Zhang, R. Tezaur, C. Farhat. The discontinuous enrichment method for elastic wave propagation in the medium-frequency regime. *Int. J. Numer. Methods Engng.* **66** (2006) 2086-2114.



# Background, Interests, Experience

([www.stanford.edu/~irinak](http://www.stanford.edu/~irinak))

## ● Education:

- Ph.D. Candidate, Institute for Computational & Mathematical Engineering, Farhat Research Group, **Stanford University**, Stanford, CA (expected June 2011).
- B.A., M.A., Mathematics, **University of Pennsylvania**, Philadelphia, PA (May 2006).

## ● Other Research Experience: Graduate Technical Intern, Aeronautics Department, **Sandia National Laboratories**, Albuquerque, NM (June 2007 – August 2010).

- Reduced Order Modeling of Fluid/Structure Interaction (Mentor: Matthew F. Barone).
- Modeling of Transitional and Fully Turbulent Pressure Fluctuation Loading (Mentor: Lawrence J. DeChant).

## Current Research Interests:

{ Finite Element Methods  
 Numerical Solution to PDEs  
 Reduced Order Modeling

